5 ΠΣΑΜΤΣ
ΑΘΗΝΑ 20-22 ΟΚΤΩΒΡΙΟΥ 2022

Assessment of stiffener spacing design requirements for intermediate EBF links via nonlinear finite element analysis

Nikolaos G. Skretas[1], **Theodoros L. Karavasilis**[2], **Dimitrios G. Lignos**[3]

ABSTRACT

Links in eccentrically braced frames (EBFs) with intermediate length are designed with transverse web stiffeners. Web stiffening is required because the common failure modes are associated with web buckling as well as flange and lateral torsional buckling. Current design stiffener spacing requirements for intermediate length have been based on preliminary work that dates back to early 1990s. This paper assesses, through nonlinear continuum finite element analyses, the stiffener spacing design requirements per AISC-341-16 of intermediate length EBF links.

Keywords: Eccentrically Braced Frames, Intermediate Links, Seismic Effects, Structural Steel

1 INTRODUCTION

Eccentrically braced frames (EBFs) concentrate inelastic deformations in a specific portion of the beam, referred to as the 'link' hereinafter. Links are classified as short, intermediate, and long based on the type of plastic mechanism developed. The three categories are shown in Fig. 1 according to AISC-341-16 [1] and EN1998-1 [2] where e is the link's length, M_p is its plastic bending moment, and V_p is its plastic shear strength. There is a difference between EN1998-1 and AISC-341-16 regarding the upper bound of intermediate length links. Hereinafter the AISC-341-16 bounds are considered for further assessment. Fig. 1 shows that the vast majority of the tested EBF links are in the short length range, whereas limited experimental data are found for intermediate ($1.6 < e/\left(M_p/V_p\right) \leq 2.6$) and long length links ($e/\left(M_p/V_p\right) > 2.6$).

Depending on the employed design and detailing criteria, the maximum inelastic rotation angle, $\gamma_{p,\max}$ of the EBF link should meet the required levels of plastic deformation capacity. Moreover, the design of the adjacent non-dissipative structural elements, is based on capacity design principles that mobilize the associated overstrength, Ω. The definitions for both $\gamma_{p,\max}$ and Ω are provided in Fig. 2a, where V_n is the nomimal strength of link, $V_n = max\{V_p; 2M_p/e\}$. The geometric parameters used herein are defined in Fig. 2b. The maximum permitted inelastic rota-

[1] Ph.D. Candidate, University of Patras, n.g.skretas@gmail.com
[2] Associate Professor, University of Patras, karavasilis@upatras.gr
[3] Associate Professor, École Polytechnique Fédérale de Lausanne (EPFL), dimitrios.lignos@epfl.ch

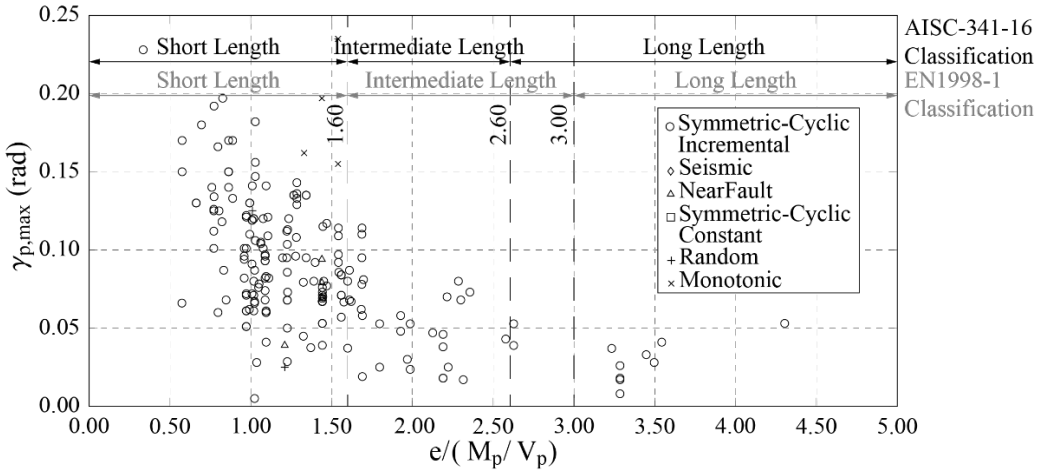

Figure 1: Attained inelastic rotation angles of 224 tested links along with the classification of links based on their dimensionless length.

tion angles for the design of intermediate length links are given as $\gamma_{pd,\max} = 0.02 + 0.06(2.6 - eV_p/M_p)$ rad.

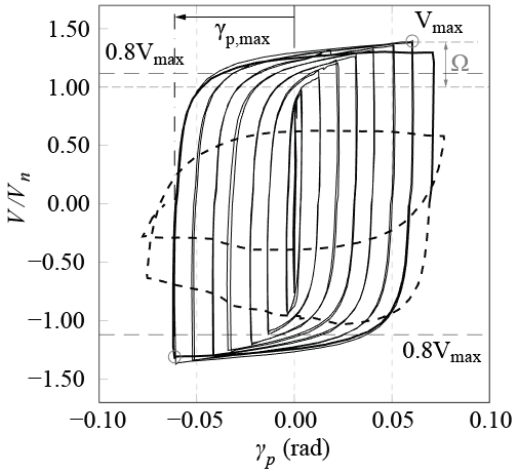

Figure 2a: Definitions of overstrength and inelastic shear distortions at 20% loss of the peak strength of links (test data from [15]).

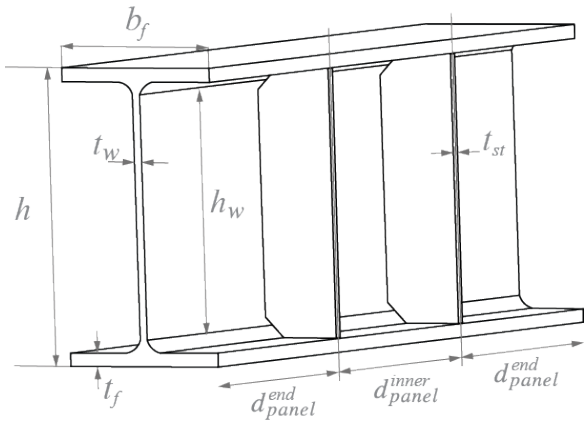

Figure 2b: Definitions of geometric parameters for EBF links.

Kasai and Popov [3] developed the stiffener spacing requirements of AISC-341-16 and EN1998-1 provisions for short links ($e \leq 1.60M_p/V_p$). Engelhardt and Popov [4] studied intermediate and long links. They recognized the differences between local geometric instabilities that are developed in long and short links. They, also, found that long links should be stiffened with transverse web stiffeners to delay both flange and lateral torsional buckling. Hjelmstad and Popov [5] tested long length links that featured A36 (i.e., nominal $f_y = 250$ MPa) W12x22 (i.e., in the range of IPE270 and IPE300 in Europe) steel cross sections. They found that the additional stiffener near the link ends nearly doubled the EBF's inelastic rotation capacity. As such, they proposed a preliminary design rule and located transverse stiffeners at a distance $1.5b_f$ away from the link ends. Conversely, for intermediate length links, since shear buckling of the web can occur along with flange buckling and lateral torsional buckling, they suggested the use of stiffener spacing requirements for long links along with the stiffening of the web within the remaining

central portion. Moreover, they noted that the use of stiffener spacing criteria for the remaining central portion of short links appears to be conservative. The above recommendations, which were not meant to be final, were only based on limited test data [6]. However, the $d_{panel}^{end} = 1.5b_f$ was adopted by EN 1998-1 and AISC-341-16 for long links. The same seismic provisions require that the web stiffener spacing of intermediate length links should meet the requirements of short and long links. As such, the maximum allowed spacing for web stiffeners in intermediate length links is expressed as follows:

$$d_{panel,max}^{inner} = \left(52 - 22\frac{\gamma_{\mathrm{pd}} - 0.02}{0.06}\right) t_w - h/5 \geq 52\mathrm{t_w} - \mathrm{h}/5 \quad (1a)$$

$$d_{panel,max}^{end} = Min\{1.5b_f; d_{panel,max}^{inner}\} \quad (1b)$$

where γ_{pd} is the targeted design inelastic shear distortion, which shall not be greater than $\gamma_{\mathrm{pd,max}}$.

Richards and Uang [7] found that many intermediate links did not achieve the required design rotation. They attributed this behavior to the associated web stiffener spacing. They also stated that (a) it seems somewhat nonconservative to extend the web stiffener spacing developed for short links to intermediate length links; and (b) the flexure–shear interaction may be appreciable at the web end panels and there they become prone to web buckling. Daneshmand and Hashemi [8] reported that some intermediate links did not meet the required inelastic rotation capacities as per the AISC-341-16 design standards [1]. They also reported that: (a) the use of double-sided web stiffeners significantly increased the rotation capacity of intermediate length links relative to their one-sided web stiffener counterparts; (b) narrowly spaced stiffeners would increase the rotation capacities of intermediate links; and (c) the $\gamma_{p,max}$ becomes sensitive to the web slenderness ratio.

In this paper we assess the stiffener spacing requirements of AISC-341-16 [1] for intermediate EBF links. The primary focus is on the evaluation of the inelastic rotation capacity of these links relative to the maximum permitted inelastic rotation capacities ($\gamma_{\mathrm{pd,max}}$). The investigation is based on numerical simulations through continuum finite element (CFE) analyses of characteristic intermediate length link geometries.

2 CONTINUUM FINITE ELEMENT MODEL

2.1 Description

The moment-shear interaction has a notable effect on the behavior of intermediate length links [4]. For some of the intermediate links, strength degradation is associated with fracture initiation and propagation due to ultra-low-cycle fatigue and/or local buckling. Herein, it is assumed that the latter prevails the EBF response.

Under the above assumption, shell elements are employed. The modelling procedures (i.e., type of element, plasticity model) comply with those from prior numerical studies on inelastic cyclic buckling of wide flange steel beams and columns [9-11]. Nonlinear geometric instabilities are properly triggered through the introduction of a combination of local and/or global imperfections.

Figure 3 depicts the boundary conditions of the CFE model. Nodes i and j are the master nodes at the link ends, whereas the nodes at the end cross sections are slaved to the master ones through a rigid constraint. The rotational degree of freedom, parallel to the transverse axis of the link, is considered fully restrained.

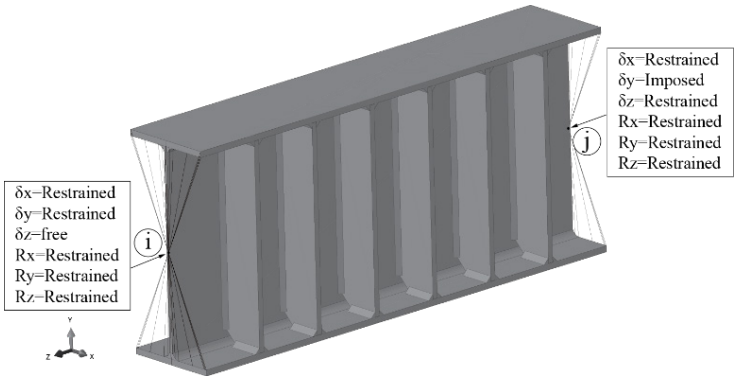

Figure 3: Boundary conditions of continuum finite element model.

In brief, quadratic 4-node doubly curved S4R shell elements were employed from the finite element library of ABAQUS 6.14 [12]. The S4R shell elements can capture the expected geometric instabilities within the cross section by incorporating the reduce integration and hourglass control formulations. The same element type can accommodate finite strains and large rotations. A structured mesh of 10 mm was used with the constraint of using up to 24 elements or more across the web height. The multiaxial plasticity material constitutive relationship by Hartloper et al. [13] is used to trace the inelastic material response. This model is developed within the framework of J2 plasticity with a combined isotropic and kinematic hardening law. Two backstresses are considered. The input model parameters are based on prior work by Hartloper et al. [13] for A992 grade 50 steel (i.e., f_y=345MPa). Local imperfections are considered by superimposing buckling modes of the bare link without stiffeners. The magnitudes of local web and flange imperfections are $h/15000$ and $b_f/15000$, respectively [11]. Furthermore, global imperfections were not considered as recommended by Hartloper [11]. Residual stresses due to hot rolling were modeled using the Young model [14]. The residual stresses were imposed only to the bare link. Residual stresses and geometric imperfections due to the welding process of stiffeners were neglected. Ductile crack initiation and propagation due to ultra-low-cycle fatigue was not considered in the CFE models.

2.2 Model validation

The proposed CFE modeling approach is validated with experimental data available in the literature. Particularly, specimen 9-RLP [15] is used for the validation of the CFE model. This specimen featured A992 grade 50 W16x36 (i.e., between IPE360 and IPE400 in Europe) cross section and had a length up to $2.0M_p/V_p$. It was subjected to the AISC-341-16 symmetric cyclic loading protocol. The specimen failed due to severe local flange and web buckling at the end panels (see Figure 4a). In-plane rotational springs with tuned stiffness are inserted at the link ends to simulate the in-plane flexibility from the surrounding test frame, which was part of the test apparatus [15].

Figure 4 shows a comparison of the simulated and experimental results in terms of the deformed shape (see Figure 4b) and the normalized shear force versus the inelastic rotation angle. The comparison suggests that the CFE model can capture the deformed shape of the EBF intermediate length link and the maximum achieved inelastic rotation angle $\gamma_{p,max}$ whereas overestimates the maximum developed shear force. At some specimens from the same test program, the bolts were tightened beforehand to fully engage the edge of the end plates and had to be retightened during the tests because they had become loose (based on private communication with Prof. Okazaki). Therefore, the CFE model represents adequately the experimental results; hence, it is employed for the assessment of intermediate stiffener spacing requirements of EBF links with intermediate length.

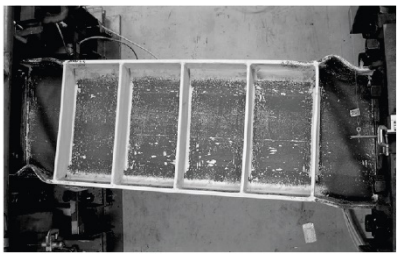

Figure 4a: Tested 9-RLP [15]

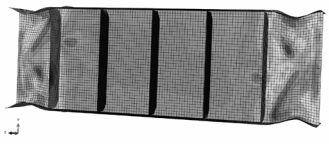

Figure 4b: Simulated 9-RLP

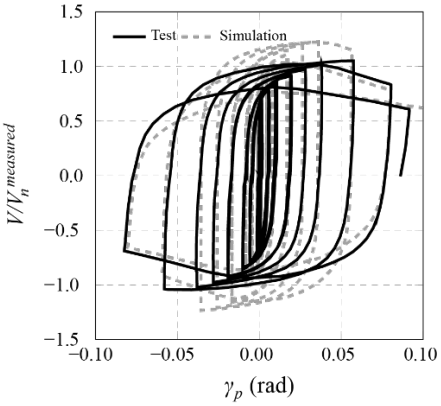

Figure 4c: Comparison in terms $V - \gamma_p$

3 SELECTED INTERMEDIATE LINKS

Table 1 shows 10 A992 grade 50 (i.e., $f_y = 345$ MPa) hot rolled EBF links for the assessment of the stiffener spacing equation of intermediate links (Eq. 1) specified in the current seismic design standards [1]. The selected links have relatively large flange width-to-thickness ratios to assess the possible flange buckling and its effect on the cyclic behavior of intermediate links. The selected links cover the range of h_w/t_w that are used in steel practice. Only links 4 and 7 are categorized as moderately ductile whereas the rest as highly ductile members according to the AISC-341-16 seismic provisions. Table 2 shows the simulated links. In the simulations single-sided stiffeners were only used. The inner stiffeners were equally spaced although AISC-341-16 do not specify that the stiffeners should be spaced in this manner.

Table 1: Geometric characteristics of short links considered for the parametric investigation.

No	Cross Section	h (mm)	h_w/t_w	$b_f/2t_f$	h/b_f	t_f/t_w
1	W21x44 (IPE450)	526	53.71	7.22	3.18	1.29
2	W21x62(IPE500-IPE550)	533	46.90	6.70	2.55	1.54
3	W16x45(IPE400)	419	42.22	6.23	2.34	1.64
4	W21x101(HEA550)	544	37.60	7.69	1.74	1.60
5	W18x86(HEA 500)	467	33.46	7.21	1.66	1.60
6	W14x68(HEA360)	356	27.42	6.94	1.40	1.73
7	W14x109(HEB360)	363	21.68	8.49	0.98	1.64
8	W14x145(HEM320)	376	16.79	7.11	0.95	1.60
9	W24x55(IPE550)	599	54.63	6.94	3.37	1.28
10	W14x82(HEB360)	363	22.35	5.91	1.42	1.68

Table 2: Simulated intermediate length links.

No.	Cross Section	$e/(M_p/V_p)$	ID	t_{st} (mm)	Intermediate stiffener distances
1	W21x44	1.70	1-1.70	10	5 @ 165 mm
		2.00	1-2.00		4 @ 223 mm
		2.25	1-2.25		2 end @ 248 mm; 2 inner @ 272 mm
		2.50	1-2.50		2 end @ 248 mm; 2 inner @ 321 mm
2	W21x62	1.70	2-1.70	11	5 @ 218 mm
		2.00	2-2.00		5 @ 257 mm
		2.25	2-2.25		5 @ 289 mm
		2.50	2-2.50		2 end @ 314 mm; 3 inner @ 325 mm
3	W16x45	1.70	3-1.70	10	5 @ 191 mm
		2.00	3-2.00		5 @ 225 mm
		2.25	3-2.25		5 @ 253 mm
		2.50	3-2.50		2 end @ 268 mm; 3 inner @ 288 mm
4	W21x101	1.70	4-1.70	13	6 @ 263 mm
		2.00	4-2.00		5 @ 361 mm
		2.25	4-2.25		5 @ 406 mm
		2.50	4-2.50		5 @ 451 mm
5	W18x86	1.70	5-1.70	13	5 @ 276 mm
		2.00	5-2.00		5 @ 324 mm
		2.25	5-2.25		2 end @ 423 mm; 2 inner @ 448 mm
		2.50	5-2.50		5 @ 405 mm
6	W14x68	1.70	6-1.70	11	5 @ 265 mm
		2.00	6-2.00		5 @ 311 mm
		2.25	6-2.25		5 @ 350 mm
		2.50	6-2.50		2 end @ 381 mm; 3 inner @ 393 mm
7	W14x109	1.70	7-1.70	14	5 @ 349 mm
		2.00	7-2.00		5 @ 410 mm
		2.25	7-2.25		5 @ 462 mm
		2.50	7-2.50		5 @ 519 mm
8	W14x145	1.70	8-1.70	18	4 @ 436 mm
		2.00	8-2.00		4 @ 513 mm
		2.25	8-2.25		4 @ 577 mm
		2.50	8-2.50		2 end @ 591 mm; 2 inner @ 675 mm
9	W24x55	1.70	9-1.70	11	5 @ 180 mm
		2.00	9-2.00		4 @ 254 mm
		2.25	9-2.25		2 end @ 267 mm; 2 inner @ 299 mm
		2.50	9-2.50		2 end @ 267 mm; 2 inner @ 352 mm
10	W14x82	1.70	10-1.70	13	4 @ 312 mm
		2.00	10-2.00		4 @ 367 mm
		2.25	10-2.25		2 end @ 385 mm; 2 inner @ 431 mm
		2.50	10-2.50		2 end @ 385 mm; 2 inner @ 507 mm

4 SIMULATION RESULTS

All the links complying to the spacing rule of Eq. 1 experienced local buckling to their end panels. This is expected when placing the stiffeners in equal distances for the cases that $1.5b_f \geq d_{panel,max}^{inner}$ due to the strong interaction between the shear-normal bending stresses at these panels. Regarding the end panels, the $1.70M_p/V_p$ links that did not meet the requirement of $\gamma_{p,max} \geq 0.074$ rad feature a d_{panel} (see Fig. 2b), which is almost equal to the maximum permitted one from Eq. 1. The other links have an applied-to-permitted d_{panel} ratio less than 0.92

except link 3-1.70 (i.e., corresponding ratio is 0.96). The applied-to-permitted ratio of the end panels for the simulated 2.00 and $2.25M_p/V_p$ links ranges from 0.85 to 0.97 and from 0.83 to 1.00, respectively. The simulated $2.50M_p/V_p$ links with the required inelastic rotation capacity have an applied-to-permitted d_{panel} ratios that ranges from 0.79 to 1.00.

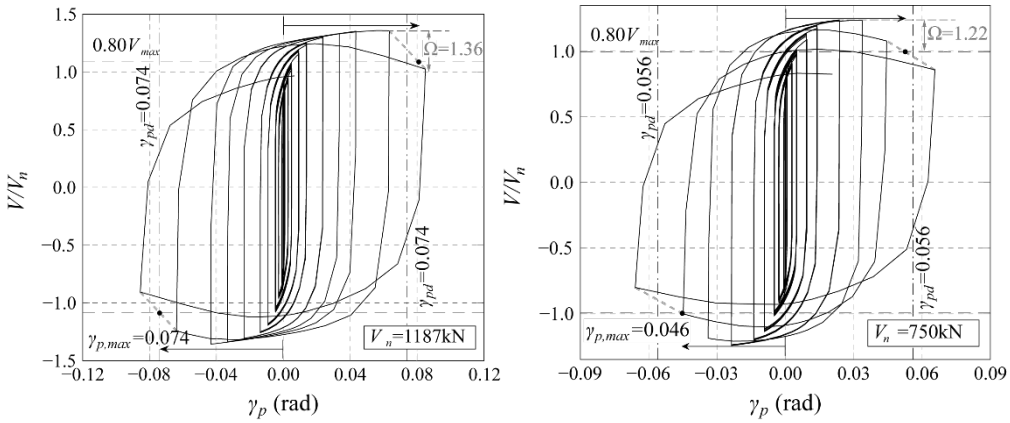

Figure 5: Representative plots of normalized shear - inelastic rotation angle (Left:Link 5-1.70, Right: Link 3-2.00).

Figure 5 shows representative $V/V_n - \gamma_p$ diagrams for some of the analyzed links along with the associated engineering demand parameters (EDPs) of interest (i.e., $\gamma_{p,max}, \Omega$). Superimposed in the same figure are the respective rotation capacity targets, γ_{pd}. Figure 6 presents collectively the outcome of the simulations regarding the above two EDPs. The links with dimensionless length 2.00 and with $h_w/t_w \geq 27$ and the links with $2.25M_p/V_p$ and $h_w/t_w \geq 46$ did not reach the maximum allowable design rotation angle due to appreciable strength degradation. The $2.25M_p/V_p$ W21x101 link with $h_w/t_w = 37.6$ did not reach the required rotation angle as well. However, this cross section is categorized as moderately ductile due to the respective flange slenderness ratio. Also $2.25M_p/V_p$ W16x45 just misses the $\gamma_{p,max}\ of$ 0.041 rad. Links 1 and 9 achieved the required inelastic rotation angle for $1.70M_p/V_p$ length but failed for the rest of the analyzed lengths. These cross sections have the highest h_w/t_w values.

Links featuring W21x62, W14x68 and W14x109 cross sections and a length of $1.70M_p/V_p$ complying to the AISC-341-16 spacing rule did not achieve the required γ_{pd}. The rest of the links achieved the required inelastic rotation capacity. Moreover, links with $2.00M_p/V_p$ developed the smallest overstrength values (see Figure 6b). It is also observed that the larger overstrength value among the links with the same cross section and different lengths corresponds to the $1.70M_p/V_p$ link. From the same figure, the resultant overstrength tends to decrease as the h_w/t_w increases due to the onset of local buckling at smaller inelastic rotation demands.

5 CONCLUSIONS

The present study aims to assess the stiffener spacing requirements of intermediate length links per AISC-341-16 [1]. The stiffener distances examined herein correspond to the maximum permitted inelastic rotation angle per AISC-341-16. The assessment is based on nonlinear continuum finite element analyses. Ten characteristic EBF geometries were examined for four

dimensionless lengths covering the intermediate length range. Seventeen (17) out of 40 intermediate length links examined herein failed to attain the required inelastic rotation angles. The simulation results suggest that end web panels develop inelastic web buckling while the rest of the panels remain practically undamaged. Highly ductile links with $h_w/t_w \leq 25$ designed according to Eq. 1 can attain the maximum permitted inelastic rotation angles. Conversely, links with $h_w/t_w > 25$ near the theoretical transition from shear to flexural behavior length (i.e., $e = 2.00M_p/V_p$) exhibit appreciable buckling at the end panels, thereby failing to achieve the required inelastic shear distortion as per the American seismic provisions.

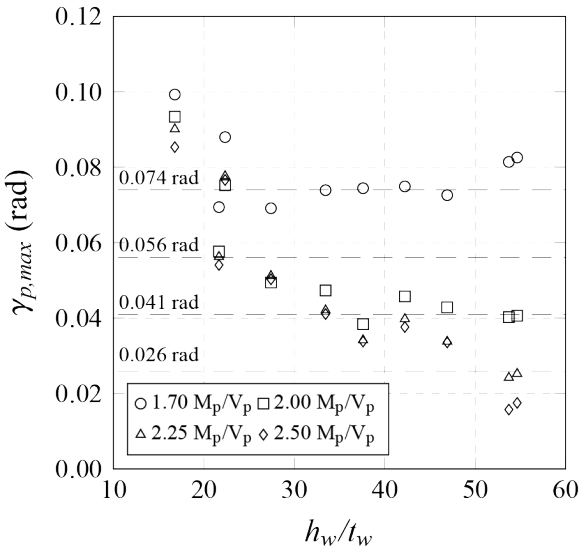

Figure 6a: $\gamma_{p,max}$ parameter of simulated intermediate links versus web slenderness.

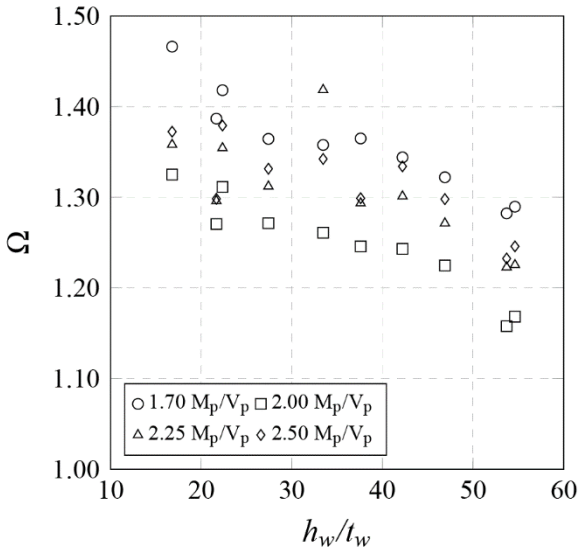

Figure 6b: Ω parameter of simulated intermediate links versus web slenderness.

6 REFERENCES

1. AISC. Specification for Structural Steel Buildings, ANSI/AISC 360-16. Chicago, IL: American Institute for Steel Construction; 2016.
2. CEN. EN 1993-1-8: Eurocode 3: Design of Steel Structures – Part 1–8: Design of Joints. Brussels, Belgium: European Committee for Standardization; 2005
3. Kasai K, Popov E. Cyclic Web Buckling Control for Shear Link Beams. *Journal of Structural Engineering* 1986; 112(3): 505–523.
4. Engelhardt M, Popov E. Experimental performance of long links in eccentrically braced frames. *Journal of Structural Engineering* 1992; 118(11): 3067–3088.
5. Hjelmstad K, Popov E. Cyclic behavior and design of link beams. *Journal of Structural Engineering* 1983; 109(10): 2387–2403.
6. Engelhardt M, Popov E. Behaviour of long links in eccentrically braced frames. Pacific Earthquake Engineering Research Center UCB/EERC-89/01 1989.
7. Richards P, Uang C. Effect of flange width-thickness ratio on eccentrically braced frames link cyclic rotation capacity. *Journal of Structural Engineering* 2005; 132(8): 1183–1191.
8. Daneshmand A, Hashemi B. Performance of intermediate and long links in eccentrically braced frames. *Journal of Constructional Steel Research* 2012; 70: 167–176.
9. Elkady A, Lignos D. Analytical investigation of the cyclic behavior and plastic hinge formation in deep wide-flange steel beam-columns. *Bulletin of Earthquake Engineering* 2015; 13(4): 1097–1118.

10. Elkady A, Lignos D. Improved seismic design and nonlinear modeling recommendations for wide-flange steel columns. *Journal of Structural Engineering* 2018; 144(9): 04018162.
11. Hartloper A. Reduced-order models for simulating coupled geometric instabilities in steel beam-columns under inelastic cyclic straining. PhD Thesis ENAC EPFL 2021.
12. Dassault Systèmes. Abaqus standard and Abaqus documention for version 6.14. Dassault Systèmes Simulia Corp., Providence, RI, USA 2014.
13. Hartloper A, de Castro e Sousa A., Lignos D.Constitutive modeling of structural steels: A nonlinear isotropic/kinematic hardening material model and its calibration. *Journal of Structural Engineering* 2021; 147(4): 04021031.
14. Young B. Residual stresses in hot-rolled members. Int. Colloquium on Column Strength, Int. Association for Bridge and Structural Engineering. Zurich, Switzerland: International Association for Bridge and Structural Engineering, 2538, 1971.
15. Okazaki T and Engelhardt M. Cyclic loading behavior of EBF links constructed of ASTM A992 steel. *Journal of Constructional Steel Research* 2007; 63(6): 751–765.